Center for Computational Sciences and Engineering
Lawrence Berkeley National Laboratory

The Modeling of a Laboratory Natural Gas-Fired Furnace with an Embedded Boundary Projection Method for Unsteady Combustion

Richard Pember
Phillip Colella
Louis Howell
Ann Almgren
John Bell
William Crutchfield
Vincent Beckner
Center for Computational Sciences and Engineering
Lawrence Berkeley National Laboratory

Keith Kaufman
Woody Fiveland
Pat Jessee
Research and Development Division
Babcock & Wilcox

Work-in-Progress Poster, 26th International Symposium on Combustion

Summary of Approach

- model for low Mach number combustion
  - equations for reacting flow, coupled with a
  - divergence constraint
- higher-order projection method: predictor/corrector
  - predictor:
    * higher-order upwind differencing of convective terms
    * Crank-Nicholson differencing of diffusive and reactive terms
  - corrector: velocity and pressure are updated using the solution of an elliptic equation derived from the divergence constraint
- projection formulation:
  - explicit convective differencing
  - time step restricted only by fluid velocity
- higher-order upwind methods
  - degrade gracefully at under-resolved gradients
  - higher-order formulation greatly reduces amount of numerical viscosity
- geometry: embedded boundary approach
  - fluid/body interface represented as a boundary embedded in a uniform rectangular grid
  - simpler grid generation and data structures, no metric terms

Model in current implementation

- axisymmetric flow
- evolution equations for
  - axial, radial, and tangential components of velocity (u, v, w)
  - enthalpy (temperature) (h, T)
  - mass fractions (Y_l)
- turbulence model: $k - \epsilon$
  - transport equations for
    * turbulent kinetic energy (k)
    * dissipation of turbulent kinetic energy (ϵ)
  - law-of-the-wall
  - coupling to evolution equations through Reynolds stresses, mass/thermal diffusivities, and eddy dissipation model
- radiation: discrete ordinates model
- kinetics: reduced mechanism
- divergence constraint

Model: Low Mach Number Formulation

- idea: if $M << 1$, acoustic waves can be "ignored"
- Pressure expressed as

$$p(x,t) = p_{amb} + \pi(x,t)$$

$$\pi / p_{amb} = O(M^2)$$

- Thermodynamic properties are independent of π
- Perfect gas law

$$\rho = \frac{p_{amb}}{R_{mix} T},$$

where

$$R_{mix} = \frac{\mathcal{R}}{W_{mix}} = \mathcal{R} \sum_l \frac{Y_l}{W_l}$$

- divergence constraint found from continuity:

$$\nabla \cdot (u,v)^T \equiv \nabla \cdot U = \frac{1}{T}\frac{DT}{Dt} + W_{mix} \sum_l \frac{1}{W_l}\frac{DY_l}{Dt} \equiv S$$

Numerical Algorithm: Summary

Steps to advance solution from t^n to t^{n+1}:

1. compute convective derivative terms $(U \cdot \nabla\phi)_{ij}^{n+1/2}$ for $\phi = u,\ v,\ T$, $(\nabla \cdot U\rho\phi)_{ij}^{n+1/2}$ for $\phi = w,\ h,\ Y_l,\ k,\ \epsilon$
   - predict half-time normal edge velocities u, v
   - do MAC-projection of edge velocities to obtain advection velocities that satisfy $\nabla \cdot U = S$
   - compute convective derivatives using higher-order upwind method
2. update ρ: $\rho_{ij}^{n+1} = \rho_{ij}^{n} - \Delta t \sum_l (\nabla \cdot \rho U Y_l)_{ij}^{n+1/2}$
3. sequentially compute $\phi_{ij}^{n+1,p}$ $(\phi = k, \epsilon, Y_l, T, h, (u^*, v^*), w)$ using Crank-Nicholson differencing of diffusive and reactive terms
   - except for ϕ, use the state at t^n as the state at t^{n+1}
   - Note: sequential approach $\rightarrow$ linear difference equations
4. compute $(\nabla \cdot q_{rad})_{ij}^{n+1}$ using discrete ordinates with $T^{n+1,p}$
5. sequentially compute ϕ_{ij}^{n+1} $(\phi = k, \epsilon, Y_l, T, h, (u^*, v^*), w)$ again using Crank-Nicholson differencing
   - except for ϕ, use $(\cdot)^{n+1,p}$ as the value at t^{n+1}
   - Note: Crank-Nicholson is repeated in order to obtain second-order accuracy in time with sequential treatment of state components
6. projection step: compute $u^{n+1}, v^{n+1}, \pi^{n+1/2}$ by using the solution of an elliptic equation to correct $u^*, v^*, \pi^{n-1/2}$

Numerical Algorithm: Projection

- note: velocity is cell-centered, pressure is node-based
- at the end of the predictor,

$$\text{have: } \frac{U_{ij}^{*,n+1} - U_{ij}^{n}}{\Delta t} = \cdots - \frac{1}{\rho_{ij}^{n+1/2}} \nabla \pi^{n-1/2}$$

$$\text{want: } \frac{U_{ij}^{n+1} - U_{ij}^{n}}{\Delta t} = \cdots - \frac{1}{\rho_{ij}^{n+1/2}} \nabla \pi^{n+1/2}$$

- obtain (Hodge decomposition) where $\delta = \pi^{n+1/2} - \pi^{n-1/2}$

$$\frac{U_{ij}^{n+1} - U_{ij}^{n}}{\Delta t} + \frac{1}{\rho_{ij}^{n+1/2}} (\nabla \delta)_{ij} = \frac{U_{ij}^{*,n+1} - U_{ij}^{n}}{\Delta t}$$

- take the divergence of both sides to obtain:

$$\nabla \cdot \left(\frac{1}{\rho_{ij}^{n+1/2}} (\nabla \delta)_{ij} \right) = \nabla \cdot \left(\frac{U_{ij}^{*,n+1} - U_{ij}^{n}}{\Delta t} \right) - \frac{S_{ij}^{n+1} - S_{ij}^{n}}{\Delta t}$$

- solve using finite-element based discretization of $\nabla \cdot \left(\frac{1}{\rho_{ij}^{n+1/2}} (\nabla \delta)_{ij} \right)$
- update:

$$\begin{aligned} U_{ij}^{n+1} &= U_{ij}^{n+1,*} - \frac{\Delta t}{\rho_{ij}^{n+1/2}} (\nabla \delta)_{ij} \\ \pi_{i+1/2,j+1/2}^{n+1/2} &= \pi_{i+1/2,j+1/2}^{n-1/2} + \delta_{i+1/2,j+1/2} \end{aligned}$$

Numerical Divergence Constraint

- the value of S is modified with a pressure relaxation term in order to account for the discrepancy between density as determined by continuity and as determined by the equation of state
- problem: the sequential approach cannot discretely guarantee

$$\rho_{ij} R_{mix,ij} T_{ij} = p_{amb}$$

  if density is defined by the continuity equation, i.e., if mass is to be conserved
- define $\tilde{p}_{ij} = \rho_{ij} R_{mix,ij} T_{ij}$
- represent $D\tilde{p}/Dt$ by $-(\tilde{p}_{ij} - p_{amb})/\Delta t$
- use continuity to obtain

$$\begin{aligned} \nabla \cdot U &= \frac{1}{T}\frac{DT}{Dt} + W_{mix} \textstyle\sum_l \frac{1}{W_l}\frac{DY_l}{Dt} + \\ & \quad f\left(\tilde{p}_{ij} - p_{amb}\right) \frac{c_{p,mix,ij} - R_{mix,ij}}{\Delta t c_{p,mix,ij} \tilde{p}_{ij}} \equiv S_{ij} \end{aligned}$$

  where $f < 1$ (for stability)

- the term $(\tilde{p}_{ij} - p_{amb})/\Delta t$ drives solution back to the constraint $\tilde{p}_{ij} = p_{amb}$

Numerical Divergence Constraint: why?

- two goals
  - keep the linear algebra linear
  - time stepping: avoid overworking a single time step
- example of difficulty if pressure relaxation is not used:
  - assume single species, $c_p \equiv 1$, $p_{amb} = \rho^n T^n$, other physical properties unity
  - update is

$$\begin{aligned} \rho^{n+1} - \rho^n &= -\Delta t \left(\nabla \cdot \rho U\right)^{n+1/2} \\ \rho^{n+1} T^{n+1} - \rho^n T^n &= -\Delta t \left(\left(\nabla \cdot \rho U T\right)^{n+1/2} + 1/2 \left(\nabla^2 T^n + \nabla^2 T^{n+1} \right) \right) \\ &= -\Delta t \left(p_{amb} \left(\nabla \cdot U\right)^{n+1/2} + 1/2 \left(\nabla^2 T^n + \nabla^2 T^{n+1} \right) \right) \end{aligned}$$

  - in order that $\rho^{n+1} T^{n+1} = p_{amb}$, must have

$$\nabla \cdot U^{n+1/2} = \frac{1}{p_{amb}} 1/2 \left(\nabla^2 T^n + \nabla^2 T^{n+1} \right)$$

  - hence, (outer) iteration is needed to enforce $\rho^{n+1} T^{n+1} = p_{amb}$
  - non-constant c_p increases complexity

Embedded Boundary Approach

- furnace wall and other surfaces are represented as a boundary embedded in a rectangular grid
  - this approach retains the "nice" features of structured grid methods while simplifying grid generation issues and avoiding metric terms
- the boundary is described by volume (Λ) and area fractions (a), and other quantities defined on irregular cells
- convective terms
  - finite-volume differencing
  - explicit differencing: possible time step limitations due to small cells
  - solution: redistribution
- diffusive terms and MAC project
  - implicit finite-volume differencing
  - redistribution of explicit viscous terms
- radiation model
- projection: finite-element based discretization

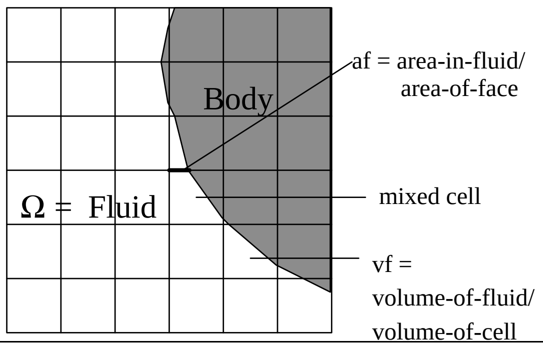

Embedded Boundary Approach: Convective Differencing

- consider model equation:

$$\frac{\partial \varphi}{\partial t} + \nabla \cdot U\varphi = 0$$

1. find reference state $\tilde{\varphi}_{ij}$ ignoring boundary

$$\frac{\tilde{\varphi}_{ij} - \varphi^n_{ij}}{\Delta t} = -\left(U \cdot \nabla\varphi\right)^{n+1/2}_{ij}$$

2. in mixed cells only,
   - compute $(\nabla \cdot U\varphi)^{n+1/2,p}_{ij}$ accounting for boundary
   - define δM_{ij} by

$$\delta M_{ij} = \left(\varphi^n_{ij} - \tilde{\varphi}_{ij}\right) - \Delta t \left(\nabla \cdot U\varphi\right)^{n+1/2,p}_{ij}$$

   - conservative (unstable) update is $\varphi^{n+1}_{ij} = \tilde{\varphi}_{ij} + \delta M_{ij}$

3. do stable (non-conservative) preliminary update

$$\tilde{\varphi}_{ij} := \tilde{\varphi}_{ij} + \Lambda_{ij}\delta M_{ij}$$

4. maintain conservation by redistributing $(1 - \Lambda_{ij})\delta M_{ij}$ to neighboring cells in a volume weighted fashion

- the above approach allows explicit convective differencing with no time step restriction due to small cells, i.e.,:

$$\Delta t = \sigma \min_{ij}\left(\frac{\Delta r}{u_{ij}}, \frac{\Delta z}{v_{ij}}\right), \sigma < 1$$

Embedded Boundary Approach: Radiative Transport

- conservative flux balance on each cell takes the form

$$\begin{aligned}\frac{\mu_{p,q}}{r_i\Delta r}(r_{i+1/2}a_{i+1/2,j}I_{p,q,i+1/2,j} - r_{i-1/2}a_{i-1/2,j}I_{p,q,i-1/2,j})+ \\ \frac{\xi_p}{\Delta z}(a_{i,j+1/2}I_{p,q,i,j+1/2} - a_{i,j-1/2}I_{p,q,i,j-1/2})+ \\ \frac{\Lambda_{i,j}}{r_i w_{p,q}}(\alpha_{p,q+1/2}I_{p,q+1/2,i,j} - \alpha_{p,q-1/2}I_{p,q-1/2,i,j})+ \\ \frac{\hat{n}\cdot\Omega_{p,q}}{r_i\Delta r\Delta z}r_w L_w I_w + k_a\Lambda_{i,j}I_{p,q,i,j} &= \Lambda_{i,j}\frac{\sigma T^4}{\pi}\end{aligned}$$

- reduces to the usual discrete ordinate discretization in fluid cells
- additional relationships between the center and edge intensities required:

$$\begin{aligned}I_{m,i+1/2,j} &= I_{m,i,j} + a_{i-1/2,j}(I_{m,i,j} - I_{m,i-1/2,j}) \\ I_{m,i,j+1/2} &= I_{m,i,j} + a_{i,j-1/2}(I_{m,i,j} - I_{m,i,j-1/2})\end{aligned}$$

- uniform isotropic flow yields equation for wall factor:

$$\begin{aligned}\frac{\mu_{p,q}}{r_i\Delta r}(r_{i+1/2}a_{i+1/2,j} - r_{i-1/2}a_{i-1/2,j}) + \frac{\xi_p}{\Delta z}(a_{i,j+1/2} - a_{i,j-1/2})+ \\ \frac{\Lambda_{i,j}}{r_i w_{p,q}}(\alpha_{p,q+1/2} - \alpha_{p,q-1/2}) + \frac{\hat{n}\cdot\Omega_{p,q}}{r_i\Delta r\Delta z}r_w L_w &= 0\end{aligned}$$

- once the intensities are obtained,

$$\nabla\cdot q_{rad} = 4k_a\sigma T^4 - k_a\sum_{p,q} w_{p,q}I_{p,q}$$

Embedded Boundary Approach: Projection

- finite element representation of δ:

$$\delta = \sum \alpha_i \chi_i$$

- χ_i's are piecewise bilinear functions equal to 1 on a single node and 0 on all other nodes
- integral representation of elliptic equation:

$$\int_{fluid} \frac{1}{\rho} \nabla\delta \cdot \nabla\chi_i r dr dz = \int_{fluid} \frac{\partial U}{\partial t} \cdot \nabla\chi_i + \frac{\partial S}{\partial t}\chi_i \; r dr dz$$

  – Note: results in a nine-point stencil in two space dimensions

- boundary conditions: $\partial\delta/\partial n = 0$ at inflow, solid walls.
  At outflow, δ is set so that there is no expansion in the radial direction
- $\nabla\delta = G\delta + (G\delta)^{\perp}$
- above is an exact projection, but we can only use

$$\nabla\delta = G\delta$$

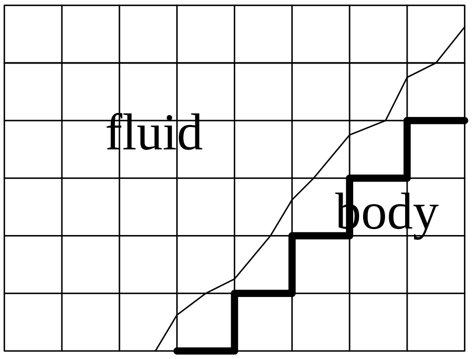

Initial validation

- BERL furnace with 300 kW IFRF burner
  - measurements were completed in the BERL at SNL as part of the GRI SCALING 400 Project under hot wall conditions
    * measurements represent "steady" operating conditions
  - we time step to a "steady-state" solution after "bootstrapping" from a solution on a reduced domain
  - simplifications/assumptions in our computation
    * axisymmetric flow
    * six species: N_2, O_2, CH_4, CO, CO_2, H_2O
    * two-step kinetics (Westbrook and Dryer)

$$\begin{aligned} CH_4 + 3/2O_2 &\rightarrow CO + 2H_2O_2 \\ CO + 1/2O_2 &\leftrightarrow CO_2 \end{aligned}$$

    * thermochemical data: JANAF tables
  - results (denoted "unsteady") are compared with measurements and with axisymmetric results previously obtained by Kaufman, Fiveland, and Jessee using a time-independent code ("steady")

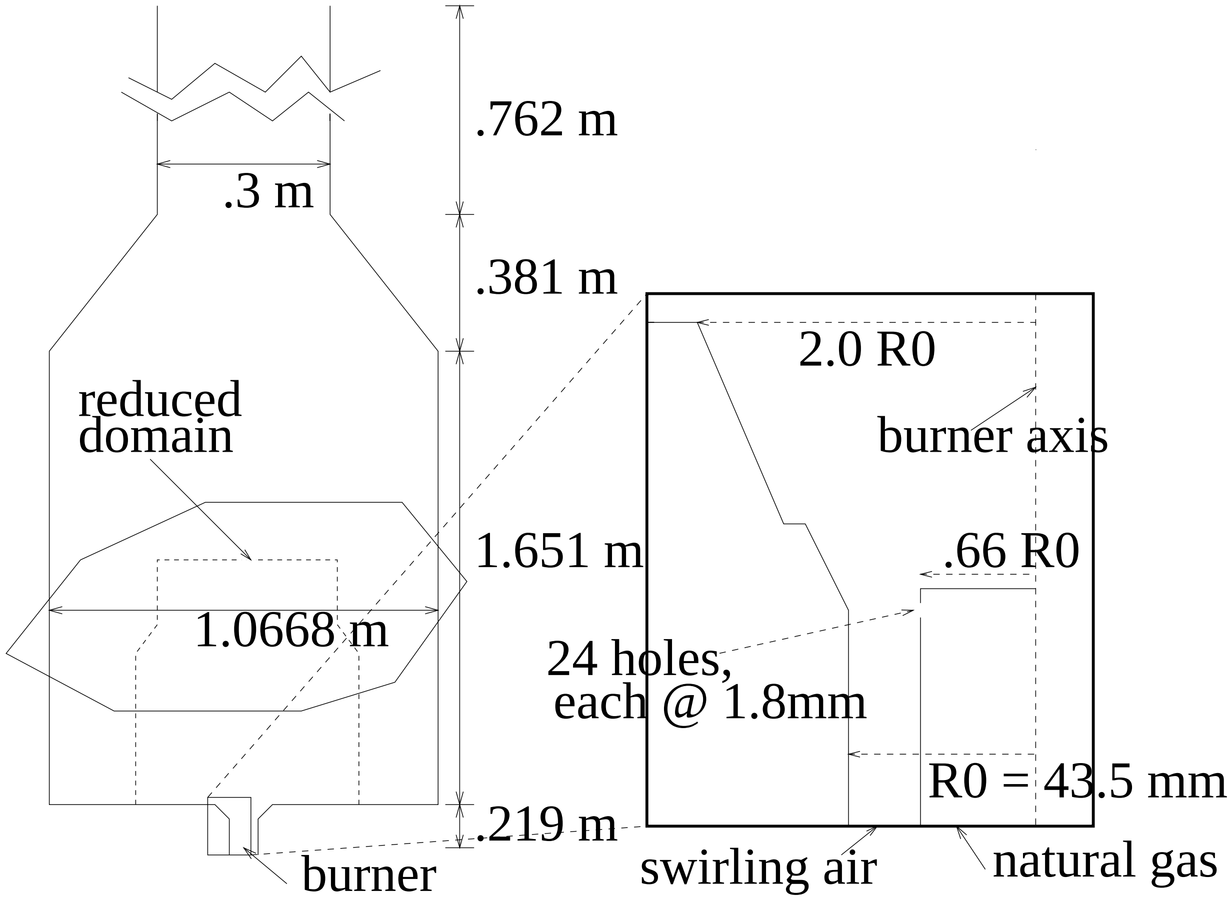

Figure 1: Sketches of the BERL furnace geometry and the IFRF 300kW gas burner geometry. The octagonal cross section is approximated as a cylindrical one. The gas injection holes in the burner are modeled as an annular slot whose height equals that of one computational cell. The gas inlet conditions are then approximated by matching the mass flow rate. The full computational domain contains only the lower .19m of the exhaust duct. The full domain is covered by a uniform 96×448 grid, i.e., $\Delta r = \Delta z = .00556$m. The reduced domain is covered by a 48×192 grid with the same grid spacing. The initial conditions in the reduced domain are no flow air at ambient temperature except for a hot patch just outside the burner throat. After 5000 time steps, the solution on the reduced domain is lifted to the full domain. The results displayed below correspond to time step 277800.

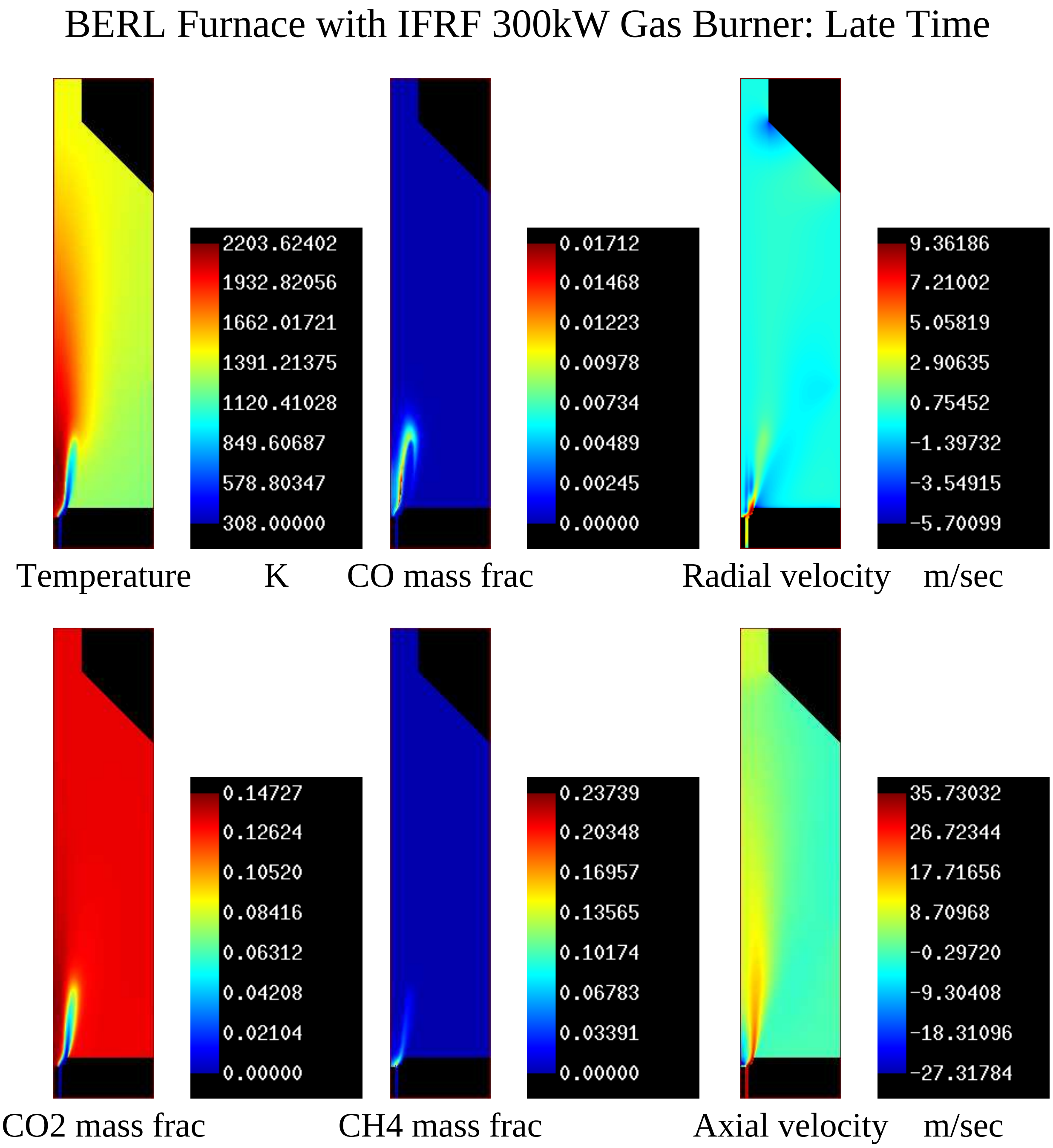

Figure 2: Temperature, velocity, and species concentrations at late time (time step 277800).

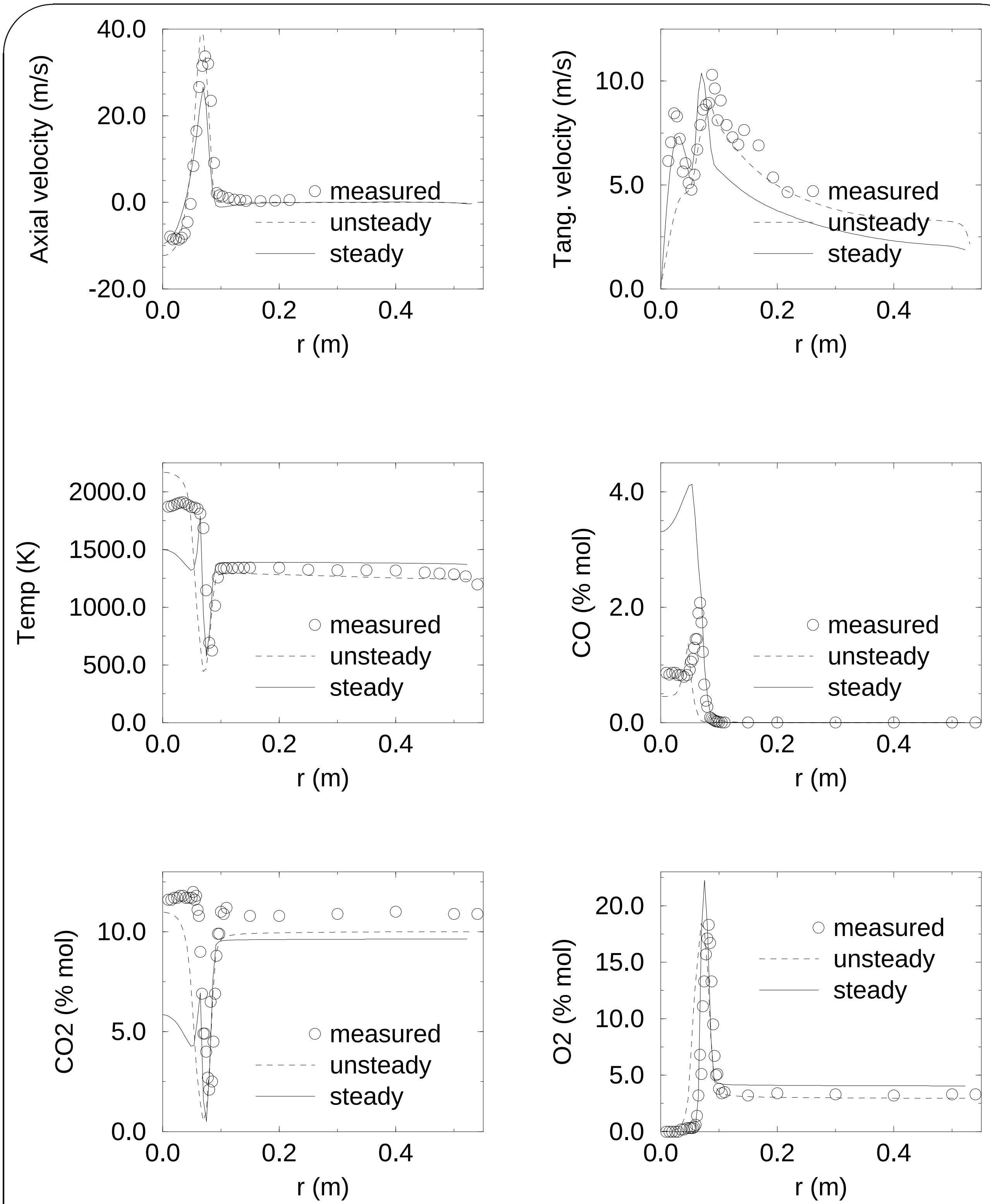

Figure 3: Radial profiles of velocity, temperature, and gas species mole fractions at 0.027m downstream of the burner throat. Species concentrations are given on a dry basis.

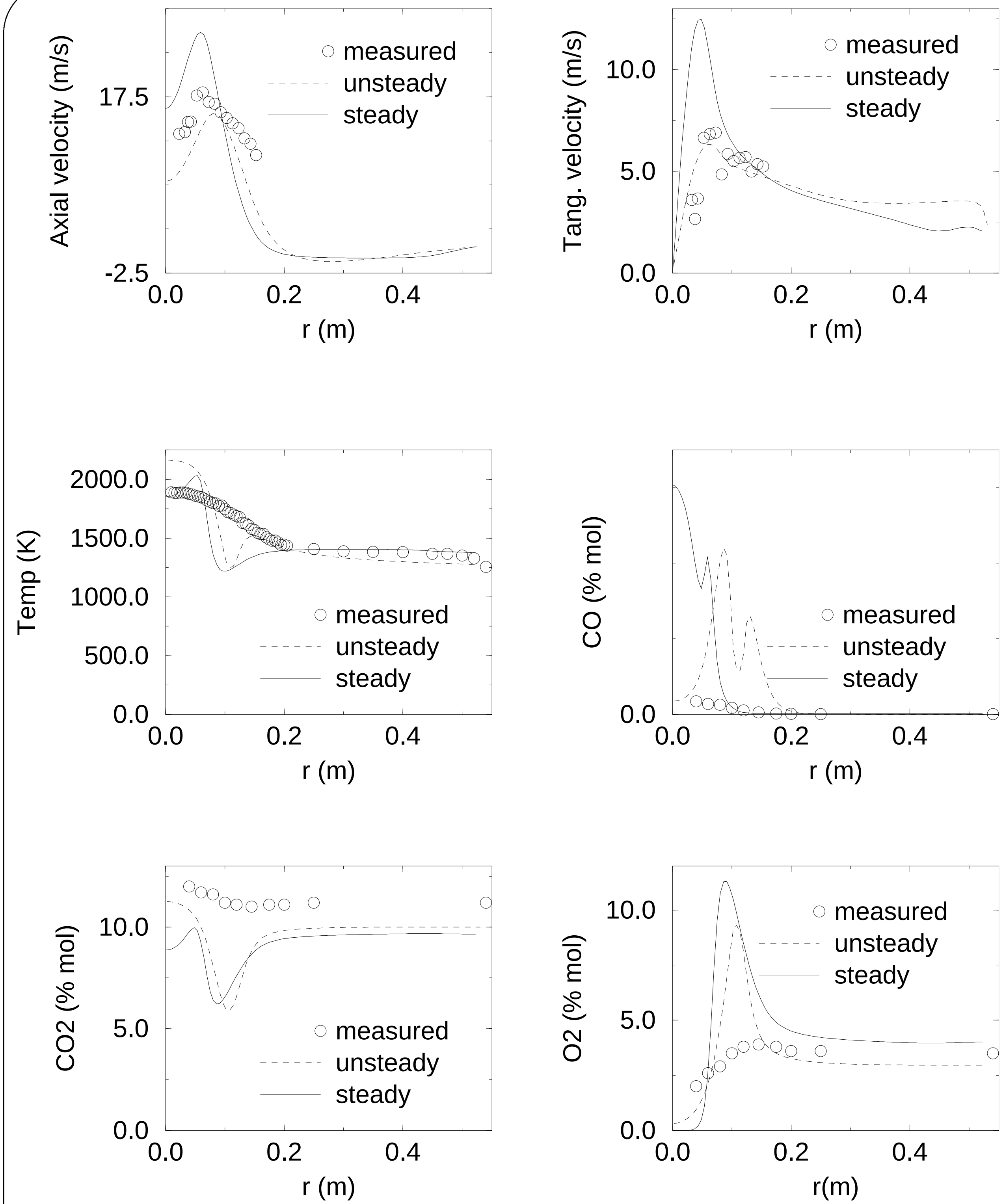

Figure 4: Radial profiles of velocity, temperature, and gas species mole fractions at 0.343m downstream of the burner throat. Species concentrations are given on a dry basis

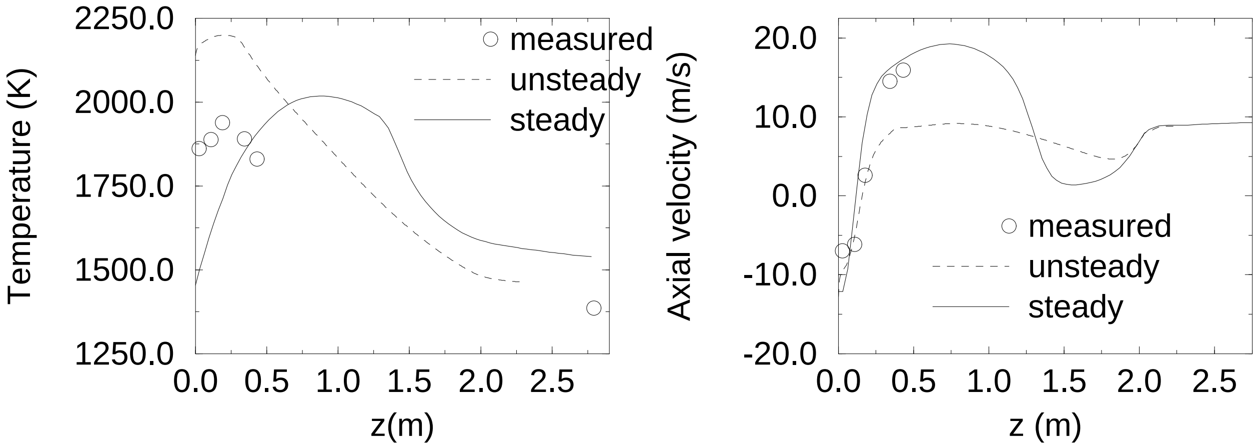

Figure 5: Measured and computed profiles of axial velocity and temperature along the burner centerline. The x-axis represents the distance downstream of the burner throat. The measured velocities are taken at 3mm off the centerline. The unsteady results represent the solution at $r = 2.78$mm.

Discussion of results

- results are encouraging, especially given comparison with steady state axisymmetric results
  - comparison suggests some discrepancy with measurements due to the axisymmetric treatment
- elongation of jet and higher temperatures in internal recirculation zone is probably due to the modeling of the fuel jet as a "conical" frustum and the lack of three-dimensional dissipation mechanisms
  - see also Peters and Weber, 1994; Kaufman and Fiveland, 1995

Discussion of results (con'd)

- high temperatures may be also be due to the use of
  - reduced mechanism; in particular, the adiabatic flame temperature of a CH4-air flame without dissociation is roughly 100 K higher than an actual methane-air flame
  - too high a rate constant in the eddy dissipation model
- in the "time-dependent" results (not shown here), the velocity too rapidly attains a "steady" character. We believe this is an artifact of the $k - \epsilon$ model. (Note that this was not the case for temperature or species.)

Additional discussion

- note that using a time-dependent method with a CFL restriction on the time step is a rather inefficient way of computing a "steady-state" flow
  - temperature and species concentrations are almost but not quite yet time-steady at step 277800
- the computation presented here was simply an initial validation, i.e., with an unsteady method it should be possible to time step to a steady-state solution if one exists
- the true benefit of our approach will be in computing unsteady phenomena under "steady" operating conditions. Such computation should ideally be three-dimensional and should employ a turbulence model better suited to time-dependent flow than the $k - \epsilon$ model

Conclusions

- we have developed an embedded boundary projection method for the modeling of low-Mach number combustion in an industrial furnace
- we have an initial implementation of the algorithm for axisymmetric flow which employs a reduced kinetics mechanism and a $k - \epsilon$ turbulence model
- as an initial validation, we have computed the "time-steady" flow in a laboratory furnace by time stepping to a "steady-state" solution

Work-in-Progress/Future Work

- more validation
- Adaptive Mesh Refinement (see Poster #195)
- 3-d
- better physics submodels
  - turbulence (LES, PDF, EDC)
  - kinetics, including NOx mechanisms
    - ultimately, full GRI-Mech natural gas mechanism
  - two-phase combustion